Electronic Supplementary Material (ESI) for Dalton Transactions.
This journal is © The Royal Society of Chemistry 2024

Supporting Information for

Polyoxometalates/s-Triazine Hybrid Heterostructures with Ultrafast Photochromic Properties

Yue-Chen Chen [a], Yi-Ming Di [a], Shu-Quan Zhang [b] and Mei-Jin Lin [a,c*]

[a] *State Key Laboratory of Photocatalysis on Energy and Environment, College of Chemistry, Fuzhou University, China, 350116.*

E-mail: meijin_lin@fzu.edu.cn.

[b] *College of Zhicheng, Fuzhou University, China, 350002.*

[c] *College of Materials Science and Engineering, Fuzhou University, China, 350116*

Table of Contents:

1. Synthesis of ligand and D-A hybrid heterostructures

A flask was charged with 4-cyanopyridine (30 g, 288 mmol, 1 equiv.) and heated to 150 ℃. Powdered NaOH (1152 mg, 28.8 mmol, 0.1 equiv.) was added to the resulting liquid and the resulting mixture was stirred at 150 ℃ for 24 h. The solid was washed with acetone (3x180 mL) and dissolved in 250 mL 2M HCl, then norit was added and sonicated for 30 min. The suspension was filtered over Celite and neutralized wit 5M NaOH (approx. 150 mL). The product was filtered and washed with water and acetone. After drying this yielded 16 g of white solid (53% yield). Spectral data are in correspondence with literature:[1] **^{1}H NMR**(400 MHz, $CDCl_3$) δ 8.93 (m, 1H), 8.56 (m,1H).

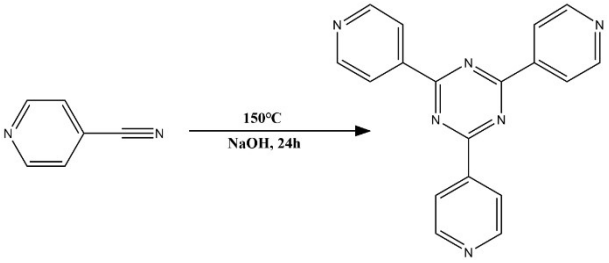

Figure S1. Scheme for synthesis of TPT.

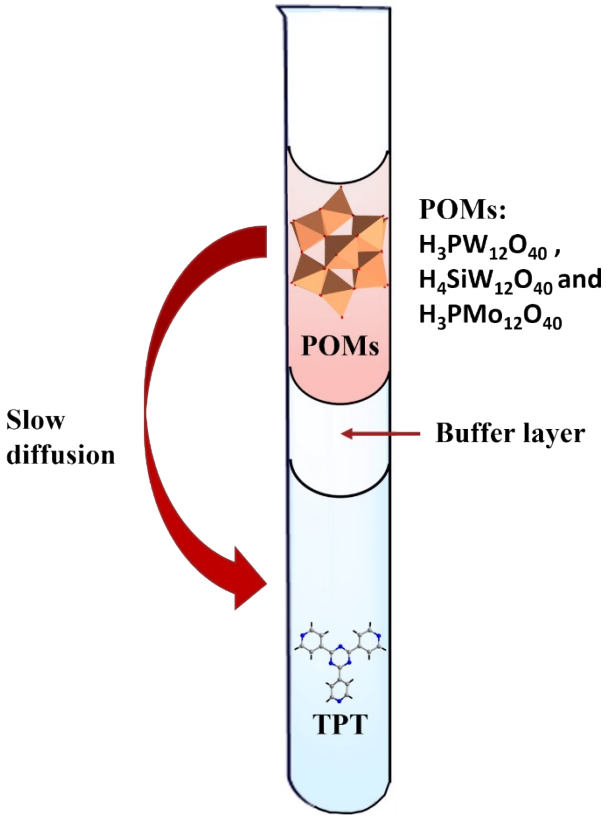

Figure S2. The synthetic scheme of four different materials.

2. Additional figures of crystal structures

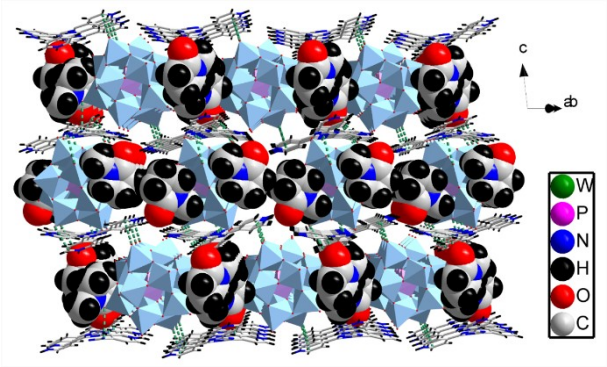

Figure S3. The 3D supramolecular structure of **1** (solvent molecules are included). The green dotted line represents anion···π interactions.

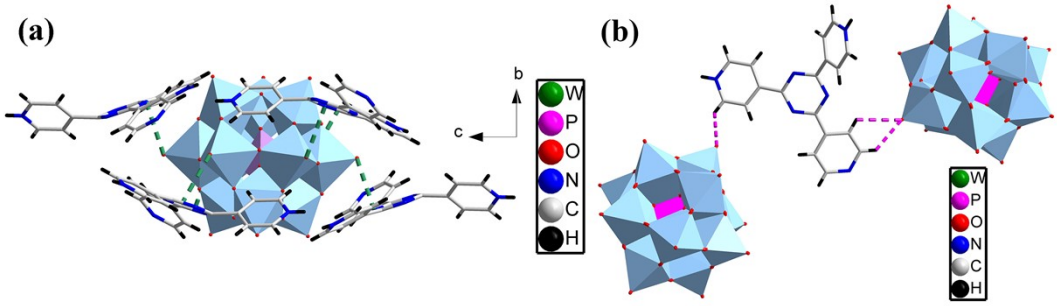

Figure S4. (a) The view of the capsule formed by $H_{1.5}$TPT ligands and the $PW_{12}O_{40}^{3-}$. (b) The C-H···O interactions between $H_{1.5}TPT^{1.5+}$ cations and $PW_{12}O_{40}^{3-}$ anions. The pink dotted line represents hydrogen-bonding interactions, and the green dotted line represents anion···π interactions.

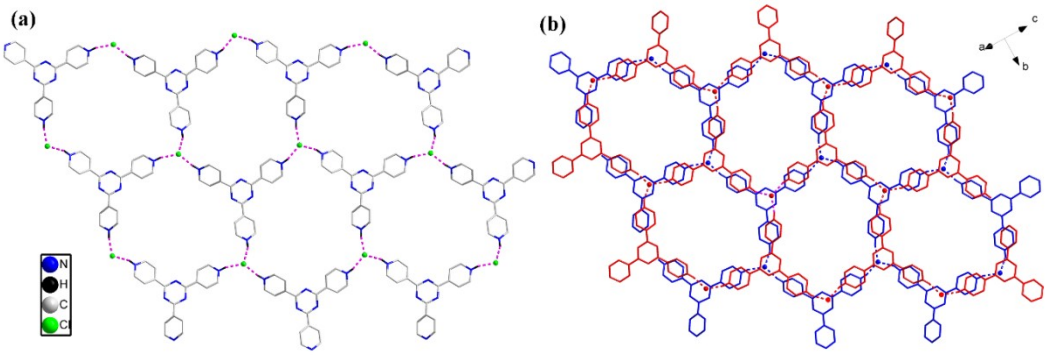

Figure S5. (a) The view of the honeycombed layers form by H_3TPT and Cl in **3**. (b) The packing mode of the adjacent layers in the (1 0 1) crystallographic plane.

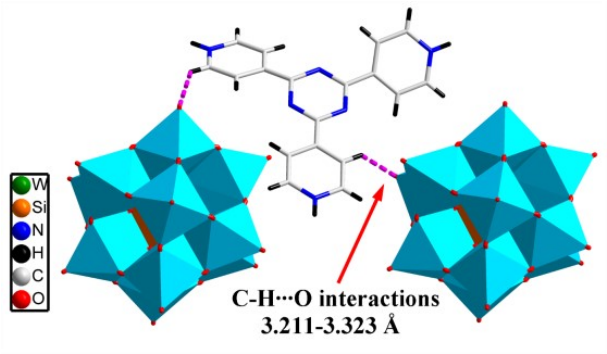

Figure S6. The C-H···O interactions between H_3TPT^{3+} cations and $SiW_{12}O_{40}^{4-}$ anions. The pink dotted line represents hydrogen-bonding interactions.

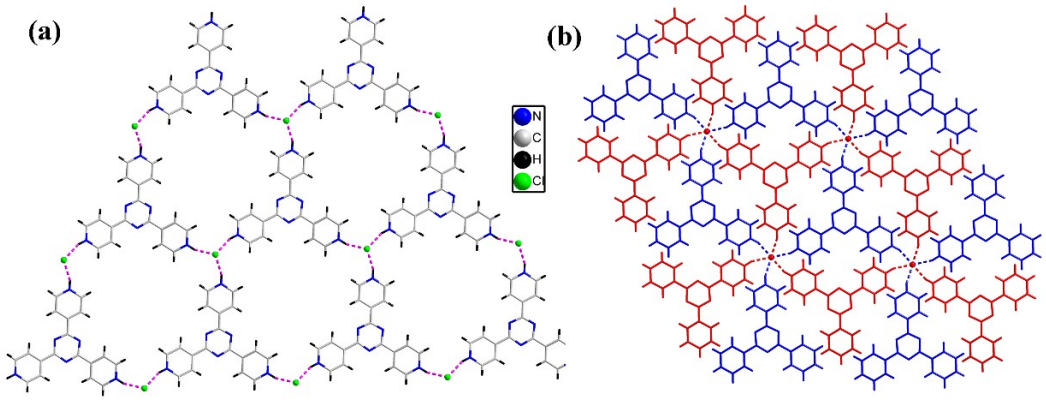

Figure S7. (a) The view of the honeycombed 2D H_3TPT-Cl layers in **4**. (b) The packing mode of the adjacent layers in the (0 0 1) crystallographic plane.

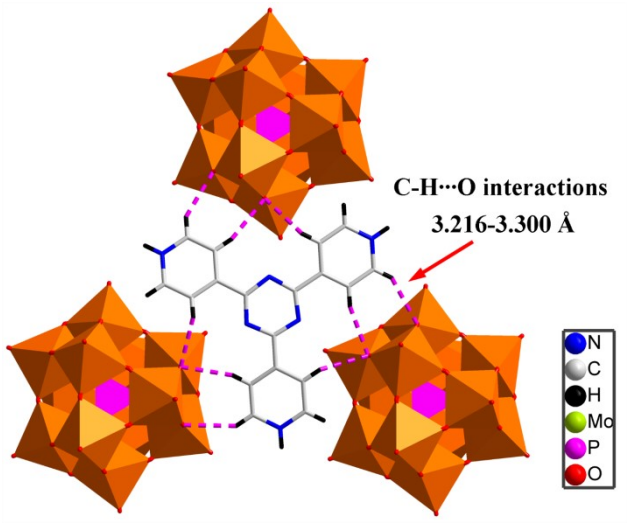

Figure S8. The C-H···O interactions between H_3TPT^{3+} cations and $PMo_{12}O_{40}^{3-}$ anions

3. PXRD spectra

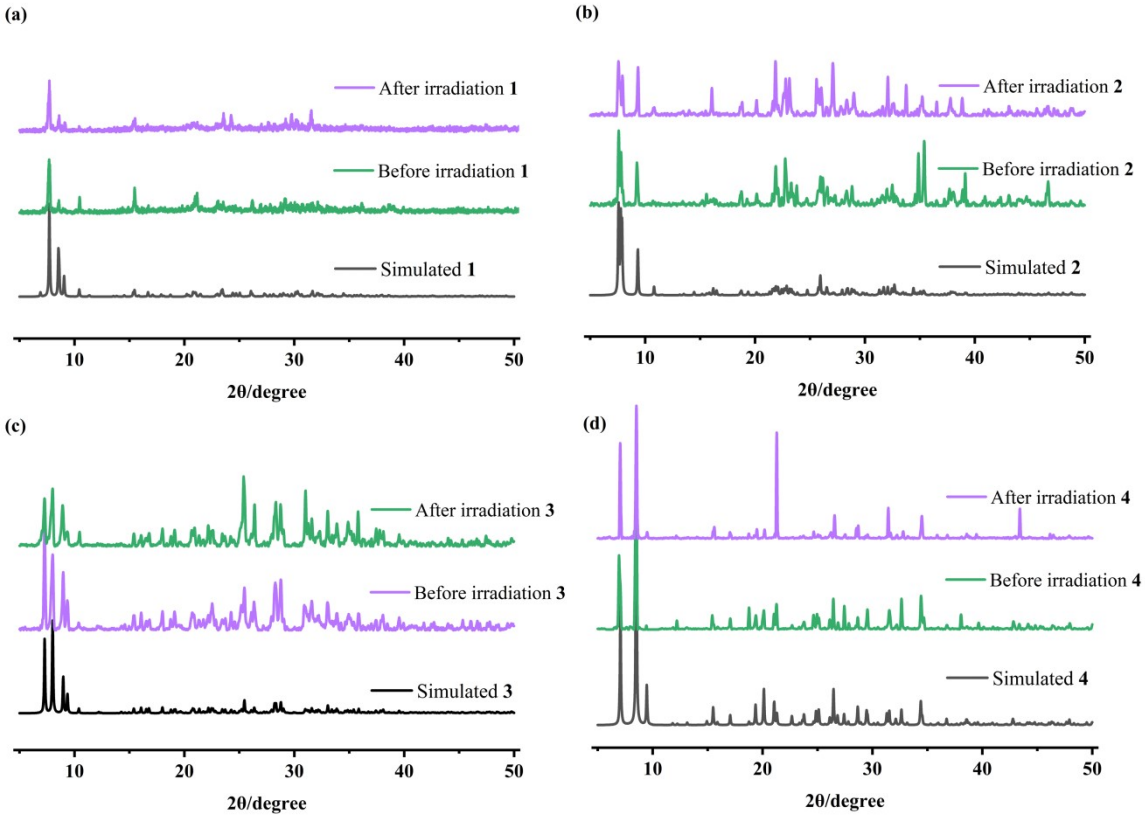

Figure S9. PXRD patterns of hybrids **1**-**4**

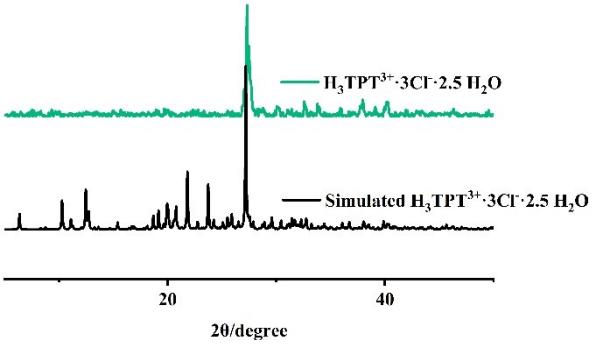

Figure S10. PXRD pattern of compound $H_3TPT^{3+}\cdot 3Cl^{-}\cdot 2.5\ H_2O$

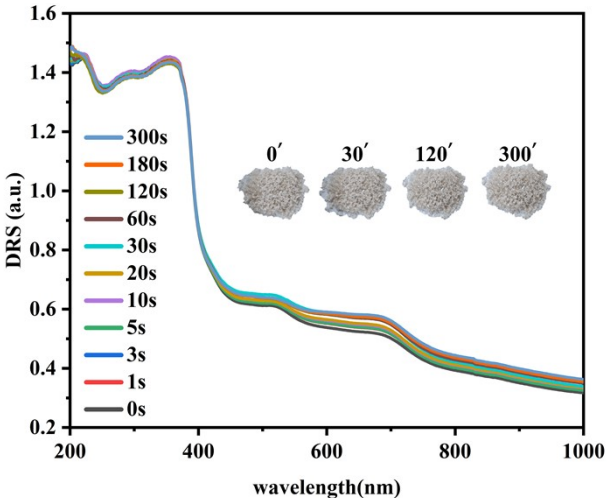

Figure S11. The solid-state diffuse reflectance spectra for compound $H_3TPT^{3+} \cdot 3Cl^- \cdot 2.5\ H_2O$ depended on the irradiation time by xenon lamp irradiation. The inserted photographs demonstrate the color changes of compound $H_3TPT^{3+} \cdot 3Cl^- \cdot 2.5\ H_2O$.

4. DFT calculations

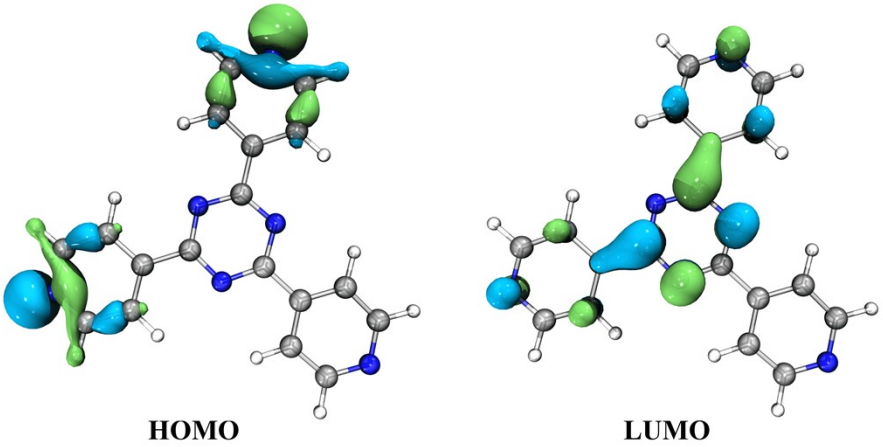

Figure S12. Molecular orbitals schemes of HOMO and LUMO of TPT

5. Infrared spectra

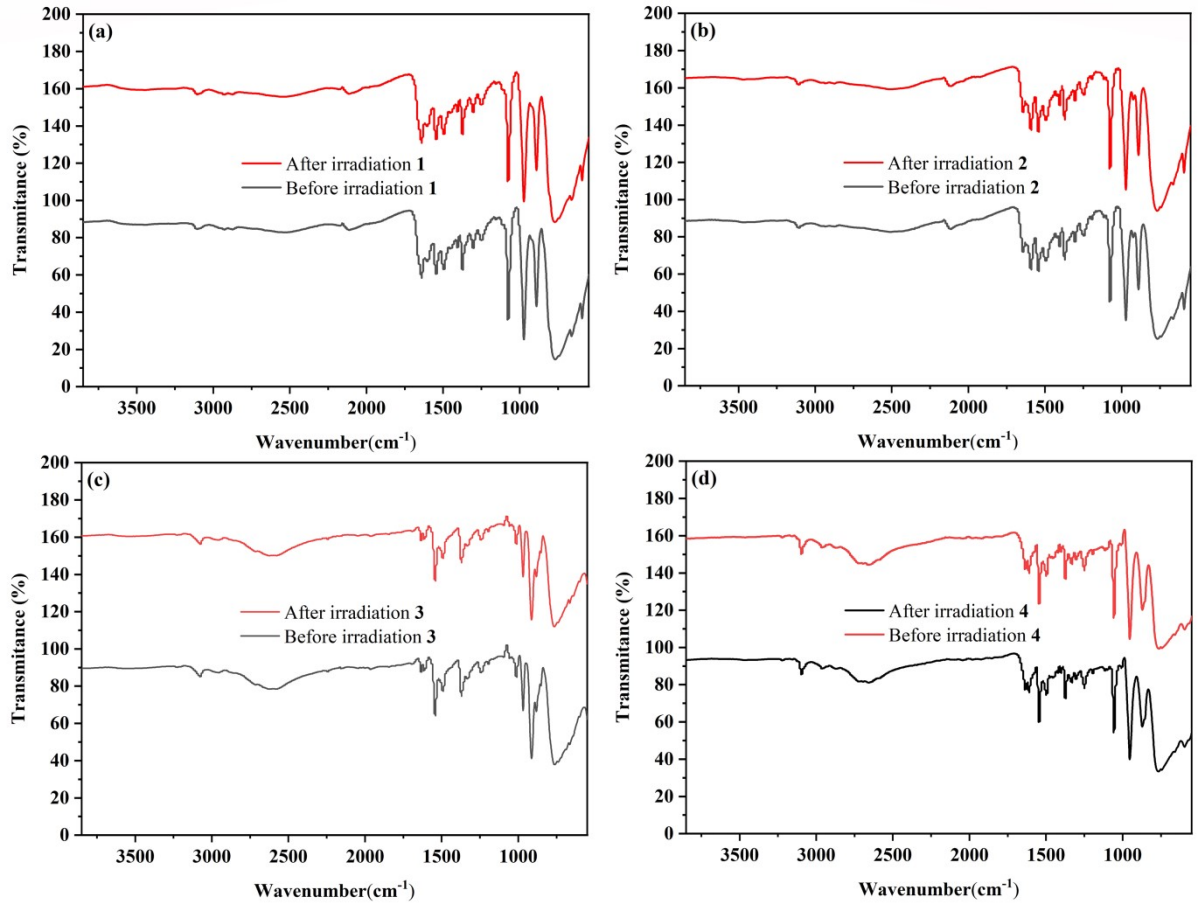

Figure S13. Infrared spectra of hybrids **1-4**

6. EPR spectra

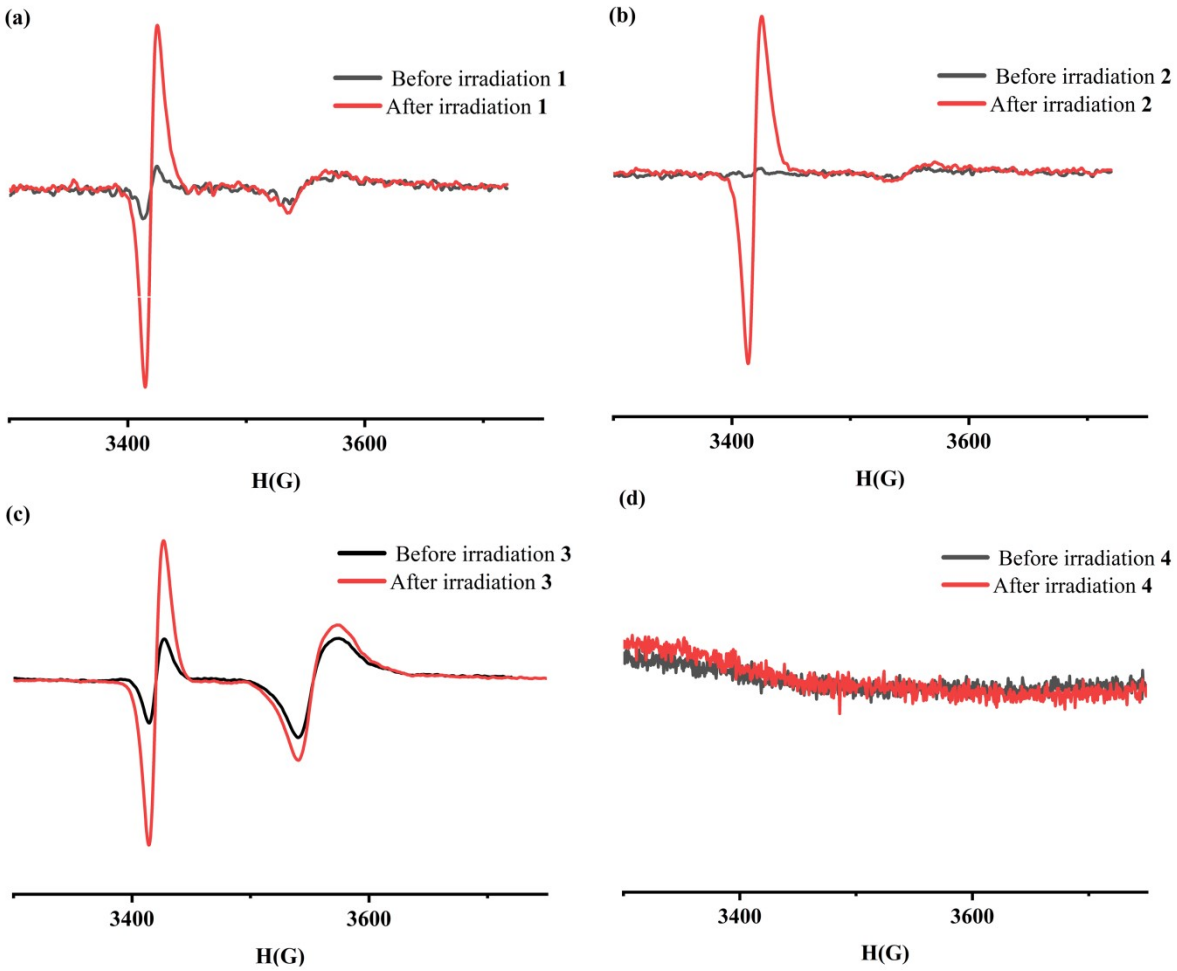

Figure S14. EPR spectra of hybrids **1-4** before and after irradiation.

7. Non-covalent interactions

Table S1. Non-covalent interactions in hybrids **1-4**

Hybrid	Anion-π		C-H···O	
	$d_{O\cdots\pi}$(Å)	Numbers[a]	$d_{C\cdots O}$	Numbers[a]
1	2.9276 - 3.0042	4		0
2	2.9695 - 3.2221	3	2.8979 - 3.3505	3
3	2.8892 - 3.2540	4	3.2110 - 3.3234	2
4	3.0522 - 3.1943	9	3.2158 – 3.3004	9

a: Only the Non-covalent interactions around one TPT are considered. No C-H···O interactions are found in hybrid **1**.

8. Crystallographic data

Table S2. 7. Crystallographic data for hybrids **1**-**4**

Complexes	**1**	**2**	**3**	**4**
Empirical formula	$C_{28}H_{36}N_8O_{42}PW_{12}$	$C_{36}H_{27}N_{12}O_{40}PW_{12}$	$C_{40}H_{36}Cl_2N_{14}O_{40}SiW_{12}$	$C_{33}H_{43}ClN_9O_{43}PMo_{12}$
Formula weight	3393.82	3504.86	3658.02	2470.45
Temperature/K	293(2)	293(2)	293(2)	293(2)
Crystal system	monoclinic	monoclinic	monoclinic	hexagonal
Space group	*C*2/*c*	$P2_1/n$	$P2_1/n$	$P6_3$
a/Å	19.8086(8)	13.2182(4)	13.8694(4)	14.4362(3)
b/Å	16.9349(6)	10.4154(3)	14.4842(4)	14.4362(3)
c/Å	20.8369(7)	22.7385(7)	17.5681(6)	18.6730(4)
α/°	90	90	90	90
β/°	99.892(3)	92.724(3)	104.594(3)	90
γ/°	90	90	90	120
Volume/Å^3	6886.0(4)	3126.94(16)	3415.34(19)	3370.16(16)
Z	4	2	2	2
ρ_{calc}g/cm^3	3.274	3.722	3.557	2.434
μ/mm^{-1}	20.068	22.103	20.316	2.318
F(000)	5996	3100	3260	2366
Reflections collected	27755	21448	27259	18893
Independent reflections	6078	5513	6031	4570
Data/restraints/parameters	6078/0/433	5513/0/467	6031/0/494	4570/0/287
Goodness-of-fit on F^2	1.041	1.037	1.182	1.165
R_1[a], wR_2[b] ($I>2\sigma(I)$)	R_1 = 0.0601, wR_2 = 0.0861	R_1 = 0.0553, wR_2 =0.1483	R_1 = 0.0530, wR_2 = 0.1043	R_1 = 0.0305, wR_2 = 0.0932
R_1[a], wR_2[b] (all data)	R_1 = 0.0410, wR_2 = 0.0921	R_1 = 0.0708, wR_2 = 0.1588	R_1 = 0.0654, wR_2 = 0.1081	R_1 = 0.0316, wR_2 = 0.0938

[a] $R_1 = \sum \big| |F_0| - |F_c| \big| / \sum |F_0|$. [b] $wR_2 = \{\sum[w(F_0^2-F_c)^2] / \sum[w(F_0^2)^2]\}^{1/2}$.